In-situ Space Environment Measurement of Near Earth and SEDA

Tateo Goka, Haruhisa Matsumoto, Kiyokazu Koga, Hideki Koshiishi, Yugo Kimoto, Yasutomo Sasaki,
Tatsuto Komiyama
Japan Aerospace Exploration Agency, Sengen 2-2-1, Ibaraki, 305-8505, Japan

ABSTRACT

The current status of measuring radiation using JAXA satellites is reviewed. Starting with Engineering Test Satellite-V (ETS-V; KIKU-5 in Japanese) in 1987, efforts to conduct radiation measurements in space have continued using almost all Japan Aerospace Exploration Agency (JAXA formerly NASDA) satellites (ETS-VI, ADEOS, ADEOS-II, MDS-1, DRTS(ongoing) and ETS-VIII(ongoing), and ALOS (ongoing)), in geostationary orbit (GEO), geostationary-transfer orbit (GTO), and low-Earth orbit (LEO). Electrons, protons, alpha particles, and heavy ions have been the main objects of study. Future plans for radiation monitoring in JAXA, including GOSAT, Jason-2 (in collaboration with CNES), and ISS/JEM/Exposure Facility/SEDA-AP, are presented.

1. Introduction

JAXA (formerly NASDA) developed TEDA (Technical Data Acquisition Equipment), which is able to measure the space radiation environment and its effects on newly developed electronic devices onboard a satellite. TEDA was designed to acquire engineering data useful to the design of future spacecraft, to diagnose the anomalies encountered on orbit, and to collect data to make new radiation belt models (electrons, protons, and alpha particles) to augment NASA radiation belt models. TEDA is composed of various instruments for every spacecraft mission. TEDA was reviewed by two papers, Kohno [1] and Fukuda et al. [2] almost ten years ago. This paper reviews current TEDA instruments and data over the past ten years, and presents our future measurement plan.

II. TEDA Post-Flight Measurement Data

TEDA instruments have flown on board ten spacecraft (Table 1). All measured data are available on the SEES (Space Environment and Effects System) website (http:// sees.tksc.jaxa.jp/).

Table 1: Spacecraft carrying TEDA

Spacecraft		ETS-V	ETS-VI	ADEOS	ETS-VII	Shuttle	ADEOS II	DRTS	ISS	MDS-1	ALOS
Launch		1987	1994	1996	1997	1998	2002	2002	2002	2002	2006
Orbit		GEO	GTO	LEO	LEO	LEO	LEO	GEO	LEO	GTO	LEO
Altitude		36k	8k-38k	800	500	400	800	36k	400	250-36k	700
DOM	DOse Monitor	◎	◎				◎	◎		◎	
HPM	High energy Particle Monitor			◎							
LPT	Light Particle Telescope										◎
HIT	Heavy Ion Telescope		◎	◎						◎	◎
DOS	DOSimeter (RadFET)			◎			◎			◎	◎
MAM	Magneto Meter		◎							◎	
AOM	Atomic Oxygen Monitor				◎						
NEM	NEutron Monitor					◎			◎		
PLA	Plasma Monitor										
POM	POtential Monitor	◎	◎	◎							
DIM	DIscharge Monitor	◎									
SUM	Single event Upset Monitor	◎	◎	◎			◎			◎	
ICM	Integrated Circuit Monitor	◎	◎								
SCM	Solar Cell Monitor	◎	◎								
COM	COntamination Monitor	◎	◎	◎							

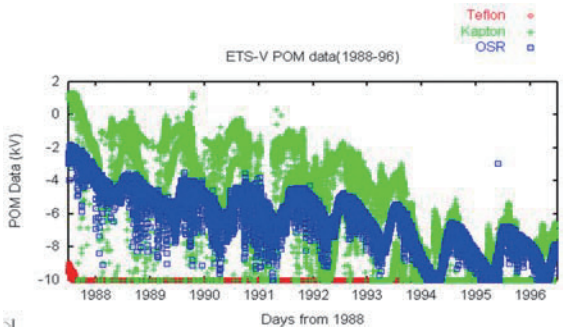

Fig. 1: POM/ETS-V measured data

2.1 KIKU-5 (Engineering Test Satellite-V) (GEO, longitude: 150 deg. E)

A dose monitor (DOM) composed of two silicon detectors was installed on this satellite [1-2]. The measurement data were gathered from August 1987 to September 1997 (ten years). Single-event latch-up data acquired by a Single-Event Upset Monitor (SUM) were reported for the first time [3].

The Potential Monitor (POM) measures differences electrostatic potential on the surface of spacecraft. Figure 1 presents the POM instrument measured data for ten years. Three samples (Teflon (lowest), Kapton (highest), and OSR(middle in y axis)) were mounted on the POM. The electric field leaking from an aperture of each sample was modulated by a chopper at 1kHz, and the electrostatic electrode detected the weak electric field. POM data shows a time-trend to decrease in figure 1.The authors think that is why the radiation damage (or/and contamination) effects a decrease of secondary electron emission yields of the cover glasses for the solar cell, or/and a decrease of photo-emission yields. We are now verifying the effects on the ground test, [4].

2.2 KIKU-6 (Engineering Test Satellite-VI) (GTO: perigee 8,600 km, apogee 38,600 km)

A DOM composed of six silicon detectors and a Magnetometer (MAM) were installed on this satellite. The data were gathered from August 1994 to July 1996. The measurement data were mainly reported in three papers [5-7]. We made the first empirical radiation belt models (electrons, protons, and alpha particles in a solar minimum period) by using this data and scientific satellite AKEBONO data [8].

2.3 MIDORI (Advanced Earth Observing Satellite (ADEOS)) (LEO-POLAR: altitude: 800 km, inclination: 98.6 deg.)

A DOM and a Heavy Ion Telescope (HIT) were installed on this satellite. The data were gathered from August 1996 to July 1997. The HIT measured the interplanetary anomalous cosmic ray (ACR), oxygen, and nitrogen, with results quite similar to those of SAMPEX (Figure 2) [9].

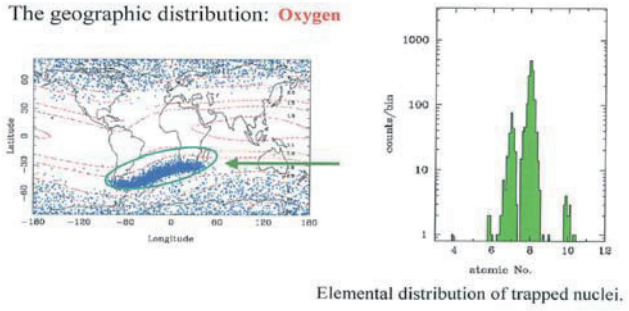

Fig. 2: Geographic distribution of oxygen and elemental distribution of trapped Anomalous Cosmic Ray (O, N, C, Ne) observed by MIDORI /HIT[9].

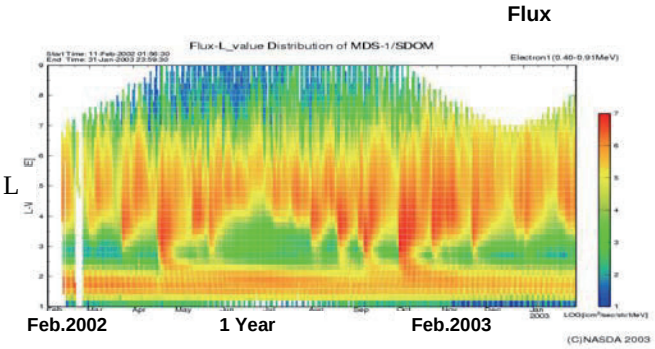

Fig. 3 : Electron Flux (0.4-0.9MeV) L-t Diagram

2.4 MIDORI-2 (ADEOS-2) (LEO-POLAR: altitude 800 km, inclination 98.6 deg.)

A DOM was installed on this satellite; data were gathered from December 2002 to September 2003[10]. The DOM data were used for diagnosis of the ADEOS-2 total loss anomaly [11].

2.5 TSUBASA (Mission Demonstration Satellite (MDS-1)) (GTO: perigee 500 km, apogee 36,000 km)

A Standard Dose Monitor (SDOM)[12], a HIT, and a MAM were installed on this satellite. The data were gathered from February 2002 to September 2003. There are many reports on these data [13-15].

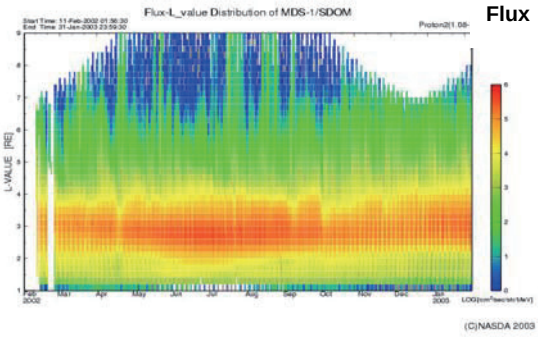

Fig. 4 : Proton Flux (1-1.5MeV) L-t Diagram

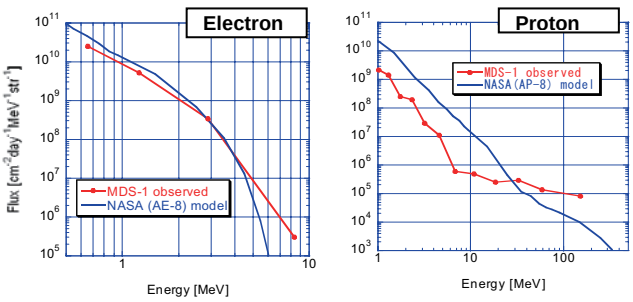

Fig. 5: Comparison between MDS-1 Observed Energy Spectrum and NASA Model

The SDOM measurement results are given in Figures 3 and 4. The electron flux (0.4-0.9 MeV) and the proton flux (1-1.5MeV) are indicated on the L-t diagram, where the vertical axis gives McIlwain's L-value ranging from L=1 to 9, and the horizontal axis gives time covering one year, starting in February 2002. Figure 5 depicts the observed and averaged electron (right) and proton (left) energy spectra, compared to the spectra calculated from the NASA AE-8 MAX[16] and AP-8 MAX[17] models, the fluxes of which were integrated along all data points of the MDS-1 orbit. The measured averaged proton fluxes were ten times lower than those of the AP-8 MAX model for energy levels below 20 MeV. However, we found that both electron and proton fluxes were broadly consistent with AE-8 MAX and AP-8 MAX models on the geomagnetic equator [18].

2.6 KODAMA (Data Relay Test Satellite; DRTS) (GEO; longitude 90.75 deg. E)

An SDOM was installed on this satellite. Data have been gathered since September 2002. Figure 6 depicts proton channel 11ch-15ch data (8MeV-211MeV) from October 2002 to January 2006. You can see 2 major peaks correspond with the Holloween Solar Flare (Oct. 2003), and the Tatina Flare (20 Jan. 2005) .

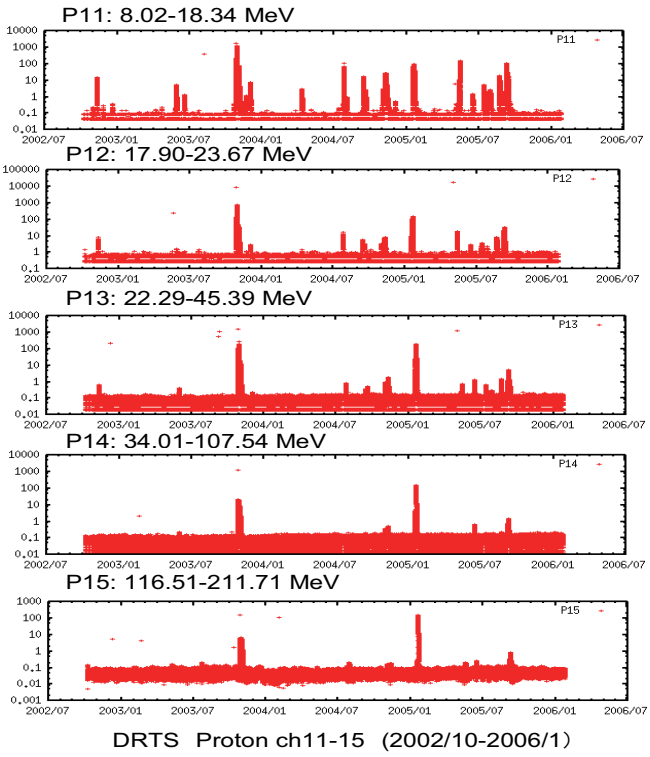

Fig. 6: Proton Ch. 11-15 (8-211MeV) data from October 2002 to January 2006, obtained by DRTS/SDOM

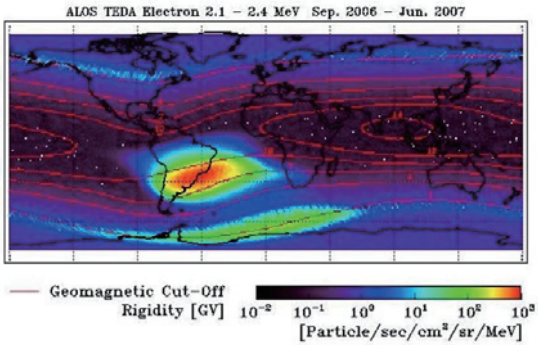

Fig. 7: LPT (ALOS) Electron (2.1-2.4MeV) 1month data (Dec.2006-Jan.2007) and geomagnetic cut off rigidity contour on a world map.

2.7 DAITI (ALOS) (LEO-POLAR: altitude 690 km, inclination 98 deg.)

TEDA consists of a Light Particle Telescope (LPT) and a HIT. Data have been gathered since February 2006. Figure 7 shows electron (2.1-2.4MeV) 1 month data and geomagnetic cut off rigidity contour on a world map, respectively. These data cleary the increased flux in the South Atlantic Anomaly (SAA).

2.8 KIKU-8 (Engineering Test Satellite-VIII) (GEO longitude 146 deg. E)

ETS-8 was successfully launched in 18, December 2006. TEDA has four components: a MAM, a POM, a DOM, and a SUM. The MAM, a fluxgate magnetometer, was placed on the upper antenna tower. The measurement range was 256, 1024, 4096, and 65536nT, the same range as that of ETS-6. The MAM data are showed in Figure 8. The POM instrument was the same instrument as ETS-V,-VI, and ADEOS, except samples. Three cover glasses (BRR/s-0213, CMX-BRR, and CMG-AR) were selected for ETS-8.

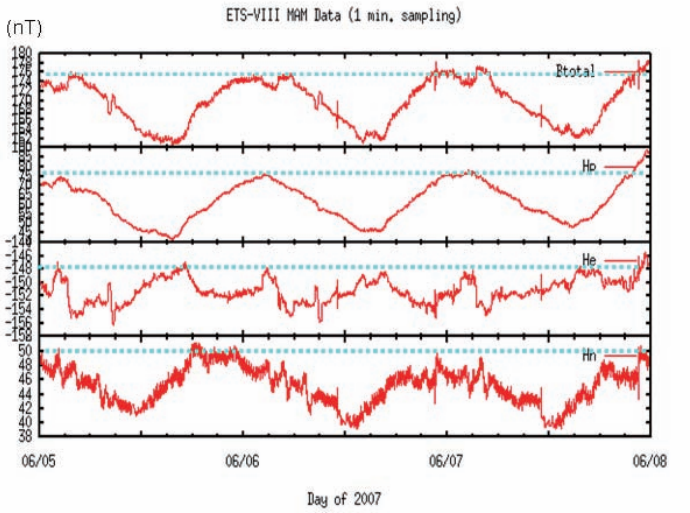

Fig. 8: Magnetometer Data (ETS-8) on 3 days (5-8, Jun. 2007), that mean B total, Hp, He, Hn, In nT, from upper to bottom panel.

III. TEDA Future Plan

JAXA are planned to be flown on various missions in the following years. Table 2 lists the confirmed TEDA mission to date.

Table 2. Planned TEDA Mission Plan

Spacecraft		ETS-8	Jason-2	GOSAT	SmartSat	ISS/JEM
Launch		2006	2008	2008	2008-2009	2008-2009
Orbit		GEO	LEO	LEO	GTO	LEO
Altitude		36k	1.3k	666		400
DOM	DOse Monitor					◎
HPM	High energy Particle Monitor					
LPT	Light Particle Telescope		◎	◎	◎	
HIT	Heavy Ion Telescope			◎		◎
DOS	DOSimeter (RadFET)	◎				
MAM	Magneto Meter	◎				
AOM	Atomic Oxygen Monitor					◎
NEM	NEutron Monitor					◎
PLA	Plasma Monitor					◎
POM	POtential Monitor	◎				
DIM	DIscharge Monitor					
SUM	Single event Upset Monitor	◎				◎
ICM	Integrated Circuit Monitor					◎
SCM	Solar Cell Monitor					
COM	COntamination Monitor					

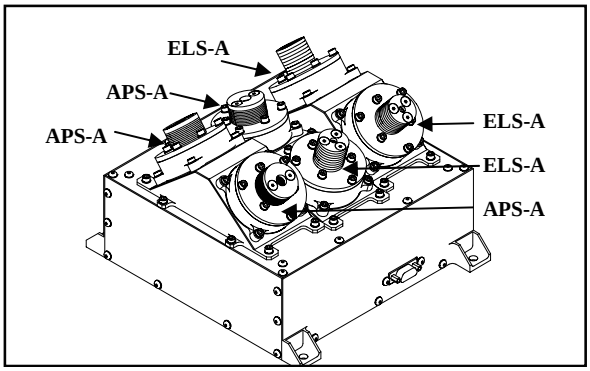

Fig. 8. LPT-3 onboard GOSAT

4.1 Greenhouse Gases Observing Satellite (GOSAT) (LEO, Polar)

GOSAT will be launched in mid-2008 into sun-synchronous sub-recurrent orbit with an altitude of 666km and an inclination of 98deg. The nominal lifetime will be five years. TEDA is composed of an LPT and a HIT. The LPT measures electron, proton, and alpha particles, and identifies the types of particles and energy. It is composed of four instruments (LPT1～4). LPT1 and LPT2 have the same configuration, composed of ELS-A, ELS-B, APS-A, and APS-B; but LPT1 and LPT2 have different fields of view. LPT3 is composed of three ELS-As and three APS-As. LPT4 is composed of APS-C [19].

Each LPT is composed of compact and high-performance sensors (Table 3). LPT3 has three fields of view to observe the distribution of pitch angle of particle flux with a geomagnetic field (Fig. 8).

Table 3 : Sensors used in LPT

Sensor	Energy range
ELS-A	Electron: 30keV～1.3MeV, 1.3MeV<
ELS-B	Electron: 280keV～20MeV
APS-A	Proton: 400keV～37MeV, Alpha: 3MeV～16MeV
APS-B	Proton: 1.5MeV～250MeV, Alpha: 20.7MeV～400MeV
APS-C	Proton: 100MeV～500MeV, Alpha: 25MeV/n～500MeV/n

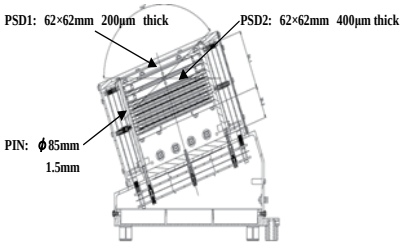

Fig. 9. HIT onvboard GOSAT

The measurement ranges of the HIT(fig. 9) are:

- He: 7～48MeV/n
- Li: 8.5～56MeV/n
- C: 13～90MeV/n
- O: 16～106MeV/n
- Fe: 28～201MeV/n.

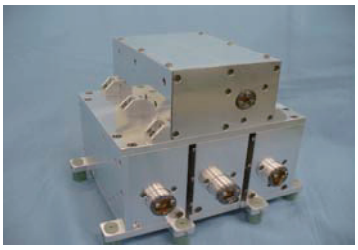

Fig. 10. LPT onboard Jason-2

4.2 Jason-2 (CNES/JAXA joint project)

CNES and JAXA agreed that the radiation particle monitor, the LPT, would be accommodated in the CNES satellite Jason-2. The mission of the JASON-2 is dedicated to ocean and climate forecasting, in continuation of the successful TOPEX-POSEIDON satellite launched in 1992 and the Jason-1 launched in 2001. Jason-2 is planned to be launched in June 2008. The altitude of its orbit will be 1,336km, and the inclination will be 66 degrees. It was decided to load the LPT on the Jason-2 with the same specifications as the GOSAT LPT1, which consists of four sensors (ELS-A, ELS-B, APS-A, and APS-B) (Fig.10) [20].

4.3 ISS JEM Exposed Facility and SEDA-AP

Development of the SEDA that will be mounted on the Exposed Facility (EF) of the Japanese Experiment Module (JEM, also known as “Kibo”) on the ISS has been completed. This payload module is called SEDA–Attached Payload (AP). The SEDA-AP will be launched by space shuttle and attached to the JEM-EF in 2008-2009. It will measure space environment data on the ISS orbit. The SEDA-AP is composed of common bus equipment that supports launch, RMS handling, power and communication interfaces

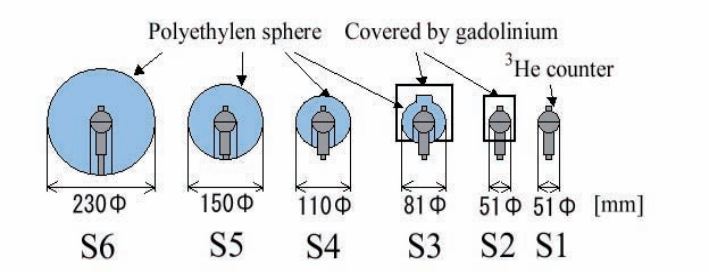

Fig。 11. A two-inch spherical He^3 proportional counter covered with a moderator of polyethylene sphere.

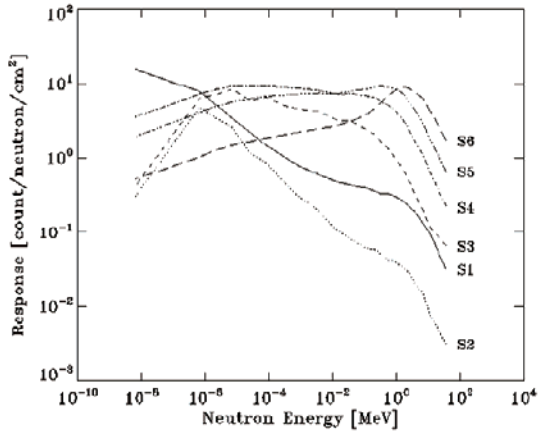

Fig。 12. Energy-response functions of each sensor for incident neutrons.

with JEM-EF, an extendible mast that extends the neutron monitor sensor 1m from the bus structure, and equipment that measures space environment data.

(1) Neutron Monitor (NM)

The NM measures the energy of neutrons from thermal to 100 MeV by two detectors, the Bonner Ball Detector (Thermal-15MeV) and the Scintillation Fiber Detector (15MeV- 100MeV) in real time. The Bonner Ball Detector discriminates neutrons from other charged particles by ^{3}He proportional gas counters, which have high sensitivity to thermal neutrons, and measures the energy of neutrons by using relative responses that correspond to different polyethylene moderator thicknesses, with the same specifications as the precursor measurements on space-shuttle (1998)and ISS inside(2001). The next paragraph shows more detail. The Scintillation Fiber Detector measures tracks of incident particles by a cubic arrangement sensor (consisting of a stack of 512 scintillator sticks), discriminates neutrons by using differences of these tracks, and measures energy of neutrons by measuring track length.

The BBND has six sensors. A two-inch spherical He^3 proportional counter is placed at the center of each sensor. Some sensors are covered with two neutron moderators as shown in Figure 11
. One is polyethylene spheres with thickness of 1.5mm, 3mm, 5mm, and 9mm, to make each sensor have different energy-response functions for incident neutrons in Figure 12. Another is a gadolinium cover with 1mm thickness in order to eliminate thermal neutrons. The energy-response functions of each sensor for incident neutrons in the assembled configuration in Figure 13 were evaluated by the numerical calculation based on the individual calibration result of each sensor obtained from irradiation experiments. The available energy range is from thermal neutron (0.025eV) through 15MeV.

The BBND hardware was launched on 8th Mar. 2001 by STS-102, and was onboard US Laboratory Module of ISS on 14th Mar. The investigation was carried out from 23rd Mar. through 14th Nov. for over eight months, corresponding to solar-activity maximum period. By applying the energy-response functions of each sensor in Figure 1 to the obtained raw data via an unfolding code NEUPAC-83[4], the differential neutron energy spectrum is obtained. Armstrong's data[5] as an initial conditions, and the assumption of the shield-thickness to be 20g/cm^2 of Alminum[6] are used in the unfolding procedure. The dose-quivqlent is also evaluated by using ICRP-74 coefficient.

Figure 14 shows the neutron energy spectrum averaged for the whole investigation period compared with the result of precursor investigation on board the STS-89[3] in 1998. The major cause of secondary neutrons inside the ISS measured by the BBND is galactic cosmic rays[7], which have the anti-correlation variation with the 11-year solar-activity. The flux obtained by the BBND is, therefore, consistently lower than that in the precursor investigation though the actual shied thickness both for the ISS and the STS-89 are not known. Figure 15 depicts the variation of the dose-equivalent rate through the investigation. The average dose-equivalent rate is 3.9 micro Sv/hour. The highest rate is 96 micro Sv/hour which appears in the SAA region. Figure 6 illustrates the distribution of the

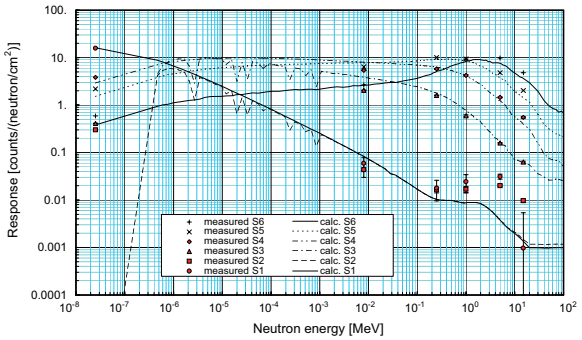

Fig. 13. Assembled configuration of the BBND sensors.

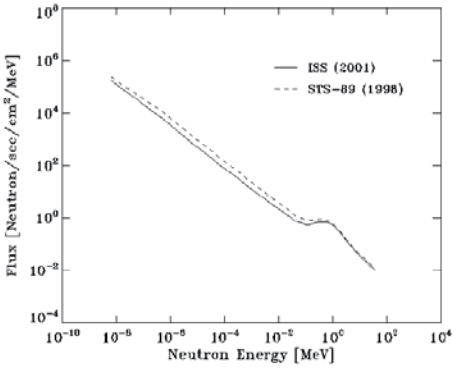

Fig. 14. Neutron energy spectrum averaged for the whole investigation period in comparison with the result of precursor investigation on board the STS-89 in 1998.

dose-equivalent rate averaged for the whole investigation period. The whole aspect of distribution is due to the geomagnetic rigidity cut off for galactic cosmic rays at the ISS orbital altitude except in the SAA region where the trapped protons cause the high rate.

(2) Heavy Ion Telescope (HIT)
The HIT uses a solid-state detector to measure the energy distribution of heavy ions (Li-Fe) that cause single-event anomalies and damage of electronic devices. The solid-state detector converts loss energy of heavy ions in the detector to electrical signals. The HIT measures incident particle mass from loss energy in each layer (delta-E) and total loss energy of each layer (E) by the delta-ExE method, with the same specifications as the ALOS.
(3) Plasma Monitor (PLAM)
The PLAM measures density and electron temperature of space plasma, which cause charging and discharging of spacecraft, by the Langmuir probe.
(4) Standard Dose Monitor (SDOM)
The SDOM measures energy distribution of high-energy light particles such as electrons, protons, and particles that cause single-event anomalies and damage electronic devices, by a solid-state detector and a scintillator, with the same specifications as the DRTS and the MDS-1.
(5) Atomic Oxygen Monitor (AOM)
The AOM measures the amount of atomic oxygen on the orbit of the ISS. The atomic oxygen interacts with the thermal control materials and paints, and lowers their thermal control ability. AOM measures the resistance of a thin carbon film that is decreased by atomic oxygen erosion.
(6) Electronic Device Evaluation Equipment (EDEE)
The EDEE measures the single-event phenomena and radiation damage of electronic parts. Single-event phenomena are induced by the impact of an energetic heavy ion or proton. The occurrence of single-event phenomena is detected by bit flips of memorized data or sudden increases of power supply current.
(7) Micro-Particles Capturer (MPAC)
The MPAC captures micro-particles that exist on orbit. Silica-aerogel and metal plates are used to capture micro-particles. After the retrieval of MPAC, size, composition, and collision energy of captured particles will be estimated.
(8) Space Environment Exposure Device (SEED)
The SEED exposes materials for space use to the real space environment. After the retrieval of SEED, degradation of these materials caused by the space environments (e.g. radiation and atomic oxygen) will be estimated.

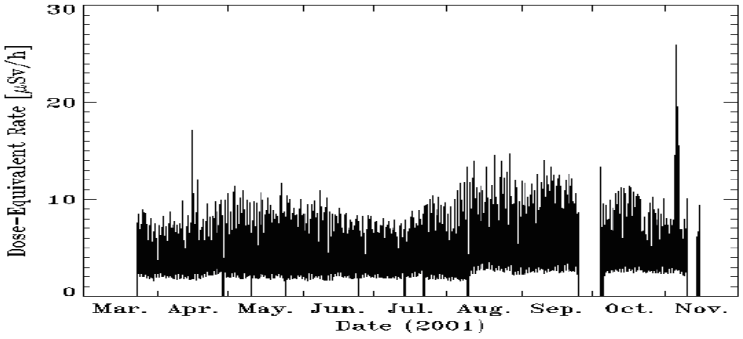

Fig. 15.　Variation of the dose-equivalent rate.

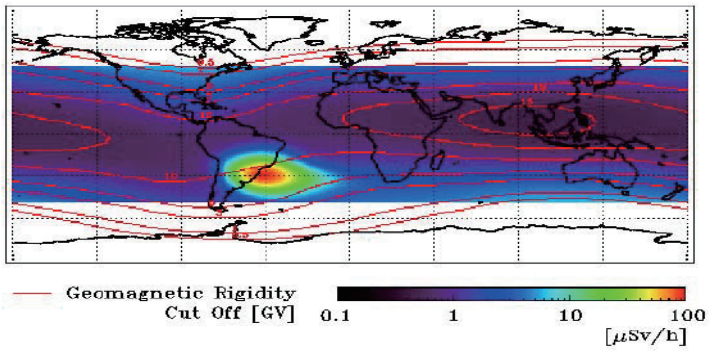

Fig. 16.　Distribution of the dose-equivalent rate averaged for the whole investigation period and overlaid with the geomagnetic rigidity cut off..

Concluding Remarks

Space environment and radiation effects measurement has been a long-term effort since 1987. Radiation monitors have been flown with almost all JAXA satellites for 20 years. This effort will be justified when new JAXA radiation belt models (electrons, protons, and alpha particles with pitch angle distributions) are developed in the very near future.

This resource will be further expanded with the instrument's flight plan on a future mission, as presented in this paper. The final goal is the creation of an international network of complementary radiation monitors providing continuous and long-term measurement of the space environment.

References

[1] Kohno, T., (1996), Current and future data available in Japan, Geophysical Monograph 97, Radiation Belts Models and Standards, J.F. Lemaire, D. Heynderickx, and D.N Baker, editors, American Geophysical Union, 217-222.

[2] Fukuda, T., T. Goka, H. Matsumoto, (1996), The Measurement of Space Environment and Effect in NASDA, IAF-96-U.3.05, 47th IAC Beijing.

[3] Goka, T., S. kuboyama, Y. Shimano, T. Kawanishi, (1991), The On-Orbit Measurement of Single Event Phenomena by ETS-V Spacecraft, IEEE Trans. On Nucl. Sci., NS-38, 1393-1699.

[4] Kawakita S., M. Imaizumi, M. Takahashi, S. Matsuda, S. Michizono, Y. Saito, (2002), Influence of High Energy Electrons and Protons on Secondary Electron Emission of Cover Glasses for Space Solar Cells, XXth International Symposium on Discharges and Electrical Insuration in Vacuum-Tours. pp. 84-87.

[5] Goka, T., H. Matsumoto, T. Fukuda, S. Takagi,(1996), Measurement of Radiation Belt Particles with ETS-6 Onboard Dosimeter, Geophysical Monograph 97, Radiation Belts Models and Standards, J.F. Lemaire, D. Heynderickx, and D.N Baker editors, American Geophysical Union, 251-254.

[6] Goka, T., H. Matsumoto, T. Fukuda, S. Takagi(1996), ,Space Environment and Effect Measurements from ETS-6 Satellite, ESA Symposium Proceedings on Environment Modelling for Space-based Applications, ESA SP-392, 51-57.

[7] Goka, T., H. Matsumoto, T. Fukuda, S. Takagi, (1996), Predictions of the Radiation Belt Particle Flux Variations from ETS-6 In-flight Measurements, Proceedings of a workshop Solar-Terrestrial Predictions-V edited by G. Heckman, K. Marubashi, M. A. Sh ea, D. F. Smart, R. Thompson, 476-479.

[8] Goka, T., H. Matsumoto, S. Takagi, (1999), Empirical model based on the measurements of the Japanese spacecraft, Radiation Measurements 30, pp.617-624.

[9] Kohno, T., H. Miyasaka, H. Kato, C. Kato, T.Goka, H. Matsumoto, (1998), Heavy Ion Radiation in Space Obseved by Japanese Satellite, Proceedings of the 3rd International Workshop on Radiation Effects on Semicinductor Devices for Space Application, 90-95.

[10] Kimoto, T., H. Matsumoto, et al, (2002), Outline of Space Radiation & Effect Monitor on board ADEOS-II, 23rd ISTS proceeding, pp.1730-1734.

[11] Goka, T., H. Matsumoto, K. Koga, Y. Kimoto,(2005), Space Environment Effects on two Satellite Anomalies in Oct. 2003 Stor m, AIAA, IAC-04-IAA.4.9.3.U.6.01, 56th IAC, Vancover,

[12] Matsumoto. H., H. Koshiishi, T. Goka, Y. Kimoto, B. D. Green, G.E. Galica,T. Nakamura, T. Abe, S. Badono,S.Murata, J. D. Sulliban, (2001), Compact, Lightweight Spectrometer for Energetic Particles, IEEE Trans. Nuclear Science, N S-48, No.6, 2043-2049.

[13] Goka, T., et al, (2002), Space Environment & Effect Measurements From The MDS-1 (Tsubasa) Satellite, 23rd ISTS proceeding, pp.1747-1754.

[14] Koshiishi, H, H. Matsumoto, Y. Kimoto, H. Liu and T. Goka, (2002), Space Environment Data Acquisition Equipment on Board Mission Demonstration Test Satellite, COSPAR Colloquia Series, Solar-Terrestrial Magnetic Activity and Space Environment, edited by H. Wang, R. Xu, pp.369-371.

[15] Kimoto, Y., H. Koshiishi, H.. Matsumoto, T.Goka, (2003), Total dose orbital data by dosimeter onboard tsubasa (MDS-1) satellite, IEEE Trans. Nucl. Sci. vol.50, No6, pp.2301-2305.

[16] Vette, J. I., (1991), The AE-8 trapped electron model environment, NSSDC/WDC-A-R&S76-06, NASA /Goddard Space Flight Center.

[17] Sawyer, D. M., Vette, J. I., (1991), AP-8 trapped proton environment for solar maximum and solar minmum, NSS DC/WDC-A-R&S76-06, NASA /Goddard Space Flight Center.

[18] Matsumoto, H., H. Koshiishi, T. Goka, (2006), MDS-1 Data Base and Radiation Belts Model, CO.1-0015-16, 36th COSPAR, Beijing China, 2006.

[19] Sasaki Y., H. Matsumoto, T. Nakamura, T. Goka, Development of Technical Data Acquisition Equipment on board GOSAT, (2006), IEICE General Conference 2006.

[20] Komiyama T., H. Matsumoto, T. Goka, JAXA/CNES Joint Radiations experiment onboard Jason-2 satellite, (2006), IEICE General Conference 2006.

[21] Bramblett, R.L., Ewing, R.I. and Bonner, T.W. (1960). A New Type Neutron Spectrometer. Nucl. Instr. and Meth. 9, 1.

[22] Lockwood, J.A. (1973). Neutron Measurements in Space. Space. Sci. Rev. 14, 663.

[23] Matsumoto, H., Goka, T., Koga, K., Iwai, S., Uehara. T., Sato, O. and Takagi, S. (2001). Real-Time Measurement of Low-Energy-Range Neutron Spectra on board the Space Shuttle STS-89 (S/MM-8). Radiat. Meas. 33, 321.

[24] Taniguchi, T., Ueda, N., Nakazawa, M. and Sekiguchi, A. (1983). Neutron Unfolding Package Code "NEUPAC-83". NEUT Research Report 83.

[25] Armstrong, T.W., Chandler, K.C. and Barish, J. (1973). Calculations of Neutron Flux Spectra Induced in the Earth's Atmosphere by Galactic Cosmic Rays. J. Geophys. Res. 78, 2715.

[26] Armstrong, T.W.and Colborn, B.L. (2001). Predictions of Secondary Neutrons and Their Importance to Radiation Effects inside the International Space Station. Radiat. Meas. 33, 229.

[27] Benton, E.R. and Benton, E.V. (2001). Space radiation dosimetry in low-earth orbit and beyond. Nucl. Instr. and Meth. B184, 255.

[28] Koshiishi, H., H. Matsumoto, A. Chishiki, T. Goka, T. Omodaka, Evaluation of the neutron radiation environment inside the International Space station based on the Bonner Ball Neutron Detector experiment, Radiation Measurenment 42 (2007) 1510-1520.